

## A novel Gold doped Cu<sub>2</sub>O photocatalyst for efficient degradation of anionic dyes

Abdussamad Mukhtar Mohammed<sup>1,2</sup>, Rohul Hayat Adnan<sup>1</sup>, Farhana Aziz<sup>3,4</sup> and Madzlan Aziz<sup>1,3\*</sup>

<sup>1</sup> Department of Chemistry, Faculty of Science, Universiti Teknologi Malaysia, 81310 UTM Johor Bahru, Johor, Malaysia

<sup>2</sup> Department of Chemistry, Yobe State University, Damaturu, Yobe State, Nigeria, Nigeria

<sup>3</sup> Advanced Membrane Technology Research Centre (AMTEC), Universiti Teknologi Malaysia, 81310 UTM Johor Bahru, Johor, Malaysia.

<sup>4</sup> School of Chemical and Energy Engineering, Faculty of Chemical Engineering, Universiti Teknologi Malaysia, 81310 UTM Johor Bahru, Johor, Malaysia.

\*Corresponding Author: [madzlan@utm.my](mailto:madzlan@utm.my)

### Article history :

Received 9 September 2020

Accepted 4 November 2020

### ABSTRACT

The photodegradation of Methyl orange (MO) and Congo red (CR) dyes was studied with pure Cu<sub>2</sub>O and composite gold doped Cu<sub>2</sub>O (Au/Cu<sub>2</sub>O) photocatalysts. A novel facile chemical reduction method at a very low temperature was used to prepare the photocatalysts. The Au/Cu<sub>2</sub>O composite shows excellent photocatalytic activities on both MO and CR, especially CR. Within 90 mins, the degradation efficiency of 99% and 79% was obtained by Au/Cu<sub>2</sub>O for CR and MO respectively. The doping effectively enhanced the separation of generated charged carriers to increased MO and CR dye degradation.

*Keywords:* Doping, composite, photocatalyst, methyl orange, congo red

© 2020 School of Chemical and Engineering, UTM. All rights reserved  
| eISSN 0128-2581 |

## 1. INTRODUCTION

Dyes can either be classified based on the method of application to the substrate as direct, reactive, vat, disperse, and azoic dyes, or based on their chemical structures like azo, anthraquinone, benzodifuranone, polycyclic aromatic carbonyl, indigoid, polymethine, styryl, aryl carbonium, phthalocyanines, quinophthalones, sulfur, nitro, and nitroso dyes. Out of all these classes, azo dyes are the most important class and constitute about 50% of the commercial dyes [1,2].

Anionic azo dyes are the most used dyes in textile industries nowadays. Methyl Orange (MO) and Congo Red (CR) are among the prominent azo dyes which have been widely used in textiles, printing, paper, leather, and plastic industries. Due to their non-degradability, the continuous use of these dyes leads to several environmental and health hazards. Azo group (-N=N-) acts as chromophore responsible for the strong color of MO and CR. With a maximum absorption spectrum of 464 and 497 nm, MO and CR have good resistance to light degradation [2–4].

For dye degradation and colored wastewater treatment, various methods have been suggested, such as coagulation-flocculation, oxidation, bioremediation, and

electrochemical processes, each of which has disadvantages that restrict their applications to some degree [5]. Photocatalysis can fully mineralize toxic compounds at low temperatures and pressure and thus, has gained much prominence in the treatment of liquid and gas wastes [6].

Copper(I) oxide or cuprous oxide Cu<sub>2</sub>O is one of the first identified semiconductors emerging as a p-type photocatalyst, it possesses the advantage of having a narrow bandgap (~2.20 eV) that enables harvesting of visible light [7–9]. Due to their abundance and low energy consumption, Cu<sub>2</sub>O nanocrystals are simple to produce, safe, low in preparation cost, they can also form a large variety of morphologies. These interesting properties make Cu<sub>2</sub>O an important metal oxide for the investigation of its catalysis and optoelectronic properties and applications. [10,11].

Cu<sub>2</sub>O application is, however, limited by fast recombination and agglomeration of electron-hole pairs. An effective charge transfer that prevents Cu<sub>2</sub>O from being self-reduced and oxidized by light is a crucial step in suppressing its recombination. Their photostability can also be increased by adding secondary components. The creation of composite materials would improve the ability of the catalyst to pass charges, reducing the excess

photogenerated charges within the particles, and thereby enhancing its photocatalytic activity [7]. To enhance the photoactivity of various photocatalysts, coupling with noble metals has proved to be effective [12].

In this work, a new facile chemical reduction method at low temperature was used to prepare Cu<sub>2</sub>O followed by modification of the synthesized Cu<sub>2</sub>O with gold (Au) nanoclusters to form Au/Cu<sub>2</sub>O. The modification successfully improved the properties of Cu<sub>2</sub>O and effectively leads to increased photocatalytic activity as well as the stability of Cu<sub>2</sub>O, this work provides insight on another strategy of improving the qualities of a photocatalyst for onward application.

## 2. EXPERIMENTS

### 2.1 Materials

Copper sulfate (CuSO<sub>4</sub>·5H<sub>2</sub>O, 99.5%), ethanol (CH<sub>3</sub>CH<sub>2</sub>OH, 99.4%), MO, and CR dye were purchased from Merck. Sodium hydroxide (NaOH, 99.4%), glucose (C<sub>6</sub>H<sub>12</sub>O<sub>6</sub>), and dichloromethane (Zn(CH<sub>2</sub>Cl<sub>2</sub>), 99.5%) were obtained from Fischer, Aldrich, and HmbG<sup>®</sup> Chemicals, respectively. AuPPh<sub>3</sub>(NO)<sub>3</sub> gold cluster was synthesized from pure gold.

### 2.2 Preparation of Cu<sub>2</sub>O particles

A simple reduction method was used to synthesize Cu<sub>2</sub>O nanostructures at relatively low temperature without the use of a microwave oven, 2.5 g of CuSO<sub>4</sub>·5H<sub>2</sub>O was dissolved in 100 ml distilled water under heating at 40 °C for 15 mins, then 3 g of glucose was added to the solution with continuous stirring until it is dissolved. Thereafter 100 ml of 0.3 M NaOH was dropped slowly and the temperature was increased to 55 °C and heated for 30 mins to produce Cu<sub>2</sub>O precipitate, the precipitate was filtered, washed with distilled water, ethanol and finally dried in the oven at 80 °C for 8 hours.

### 2.3 Preparation of Gold-doped Cu<sub>2</sub>O (Au/Cu<sub>2</sub>O)

Bis(triphenylphosphine) gold nitrate ([Au<sub>9</sub>(PPh<sub>3</sub>)<sub>8</sub>](NO<sub>3</sub>)<sub>3</sub>) otherwise known as Au<sub>9</sub> nanoclusters' synthesis followed the procedure reported by Adnal et al., (2015) [13]. 0.65 g of Cu<sub>2</sub>O was suspended in 20 ml dichloromethane under vigorous stirring, followed by drop-wise addition of Au<sub>9</sub> solution (1.8 mg in 10 ml dichloromethane) at room temperature. The mixture was left under vigorous stirring for 2 hours. The obtained Au/Cu<sub>2</sub>O was centrifuged (5000 rpm, 5 minutes) and dried in the oven at 80 °C for 4 hours.

### 2.4 Characterization

The crystallinity of the prepared Cu<sub>2</sub>O and Au/Cu<sub>2</sub>O were analyzed using the Rigaku Ultima IV X-ray diffractometer (XRD) under Cu K $\alpha$  radiation. Field Emission Scanning Microscope (FESEM) was used to study the morphology of the samples. Infrared spectra were obtained by Shimadzu Fourier transform infrared (FTIR) spectrometer (Japan) using the method of KBr pellets. Shimadzu UV-2550 spectrophotometer (Japan) was used to obtain the absorption and reflection for determining the bandgaps of the samples. The photoluminescence (PL) spectra were obtained from Hitachi F-7000 fluorescence (Japan) spectrophotometer at ambient temperature.

### 2.5 Photocatalytic experiment

The photocatalytic activity on MO and CR degradation was observed by adding 100 mg of photocatalysts into 100 mL MO and CR solutions. Adsorption studies were conducted for 30 min in the dark. Next, a 100 W LED lamp was switched on to begin photocatalytic degradation. At regular intervals, 5 mL volume of the solution was collected and filtered using a nylon-membrane syringe filter (0.45  $\mu$ m) to determine the remaining dye concentrations, monitored by Shimadzu UV-2550 spectrophotometer (Japan). The degradation of MO and CR was obtained by the change of concentration/absorbance in the MO and CR solution.

## 3. RESULTS AND DISCUSSION

### 3.1 Photocatalytic performance of Cu<sub>2</sub>O and Au/Cu<sub>2</sub>O composite

The Cu<sub>2</sub>O and Au/Cu<sub>2</sub>O were synthesized by the chemical reduction method. The photocatalysts' performance on MO and CR degradation was measured under visible light at the maximum absorption of  $\lambda = 462$  and 497 nm for MO and CR respectively. The percentage degradations were obtained from the UV-vis absorbance. In each case, the solution was first stirred for 30 minutes in the dark before turning the light on. Similarly, without the photocatalysts, a photocatalytic test was done to observe the impact of light on CR degradation by irradiating the dye solution for 4 h.

Fig. 1(a) shows the results of the photodegradation and photolysis tests of MO under visible light, 1g/L catalyst dosages under 20 mg/L initial dye concentrations were used in each case. The Au/Cu<sub>2</sub>O sample shows improved photocatalytic activity than the pristine Cu<sub>2</sub>O, within 2 hours the degradation almost reached 100% as compared to the pristine Cu<sub>2</sub>O with just 47% after 2 hours. This result is due to the Au cluster loading onto Cu<sub>2</sub>O, which formed an efficient composite photocatalyst with less recombination of charges. Likewise in Fig. 1(b) that shows the result of the photodegradation and photolysis

tests of CR under visible light, the effect of Au loading can be seen more on the degradation of CR as the dye was degraded within 1 hour of the photocatalytic test. It is worthy of note that during the first hour of the photocatalytic degradation experiment using pristine Cu<sub>2</sub>O, rapid degradation was noticed after which the degradation became slow as shown by the recorded absorbance during the experiment, this may be attributed to the inactivation of the Cu<sub>2</sub>O photocatalyst as a result of recombination of electrons and holes, this phenomenon was not seen when using Au/Cu<sub>2</sub>O, this revealed that with the formation of Au/Cu<sub>2</sub>O composite efficient charge separation was achieved leading to enhanced photocatalytic activity, similar enhancement was reported in the literature when Au is used in forming a composite photocatalyst [14].

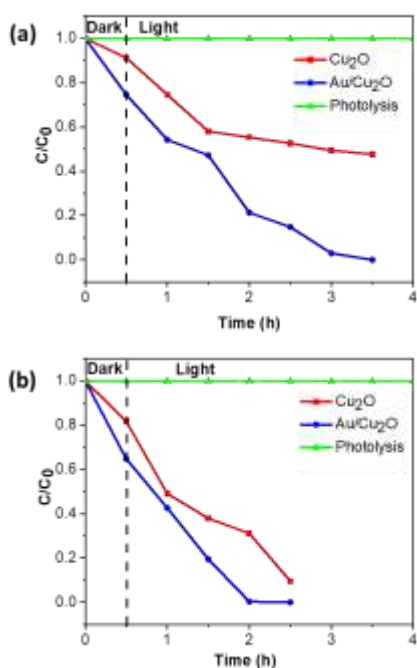


Fig. 1 Photocatalytic performance of (a) MO dye degradation and (b) CR dye degradation under visible light

Table 1 Photocatalytic degradation of MO dye by Cu<sub>2</sub>O and Au/Cu<sub>2</sub>O photocatalysts at 20 mg/L under visible light irradiation

Sample	Degradation efficiency (%)					
	30 min	60 min	90 min	120 min	150 min	180 min
Cu <sub>2</sub> O	25	42	45	47	51	52
Au/Cu <sub>2</sub> O	46	53	79	85	97	100

Table 2 Photocatalytic degradation of CR dye by Cu<sub>2</sub>O and Au/Cu<sub>2</sub>O photocatalysts at 20 mg/L under visible light irradiation

Sample	Degradation efficiency (%)					
	30 min	60 min	90 min	120 min	150 min	180 min
Cu <sub>2</sub> O	51	62	69	90	100	100
Au/Cu <sub>2</sub> O	57	81	99	100	100	100

### 3.2 XRD analysis

The structure and crystallite size of the synthesized samples were identified using XRD analysis. Fig. 2 illustrates the Cu<sub>2</sub>O, Au/Cu<sub>2</sub>O as well as the standard XRD pattern of Cu<sub>2</sub>O. In both Cu<sub>2</sub>O and Au/Cu<sub>2</sub>O, the peaks at  $2\theta = 29.4^\circ, 36.3^\circ, 42.1^\circ, 52.2^\circ, 61.1^\circ, 73.1^\circ,$  and  $77.0^\circ$  correspond to the cuprite crystal plane (110), (101), (200), (211), (220), (311), and (222), respectively, confirming the purity of both samples. Such peaks are indexable to JCPDS No. 5-667 of the Cu<sub>2</sub>O cubic structure. However, for the Au<sub>9</sub>/Cu<sub>2</sub>O samples, peaks associated with gold clusters are invisible due to the extremely low loading of gold, this was reported by Chen and his coworkers [15]. The calculated loading for gold in the Au<sub>9</sub>/Cu<sub>2</sub>O sample was 0.27 wt%, much lower than the limit of detection by X-ray diffractometer [14]. Meanwhile, the high and sharp peaks of diffraction show that the Cu<sub>2</sub>O and Au/Cu<sub>2</sub>O were well crystallized.

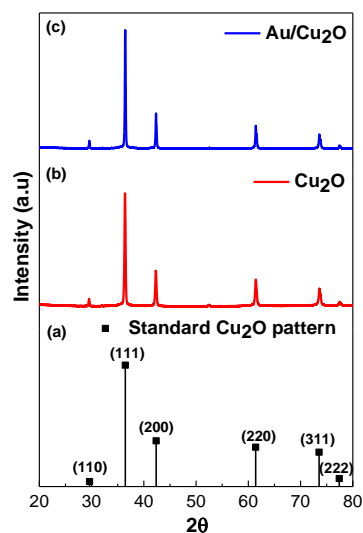


Fig. 2 XRD patterns of (a) of standard Cu<sub>2</sub>O (b) synthesized Cu<sub>2</sub>O and (c) synthesized Au/Cu<sub>2</sub>O

Using the three most intense peaks from the XRD through the Debye-Scherrer equation, the average crystallite sizes of Cu<sub>2</sub>O and Au/Cu<sub>2</sub>O were estimated. The calculated average crystallite size of Cu<sub>2</sub>O was 60 nm while for Au/Cu<sub>2</sub>O it was found to be 75 nm.

### 3.3 Structural analysis

Representative FESEM images of Au/Cu<sub>2</sub>O particles are shown in Figure 3 (a), (b), and (c) at low (2.5 kx), and high magnification, respectively. The morphology consists of predominantly quasi-spherical nanoparticles and a small fraction of nanocubes. Analysis of particle size distribution revealed high polydispersity of the sample with the size range between 300 and 1800 nm, as illustrated in the histogram of the particle size distribution in Fig. 3(d). The average particle size is calculated to be 300 nm. Such high polydispersity is commonly encountered in mixed solution Cu<sup>2+</sup>/NaOH/glucose systems [16]. Sun et al. [17] reported that large aggregated Cu<sub>2</sub>O particles result from the aggregation of much smaller Cu<sub>2</sub>O nanocubes that act as a seed. In our work, we deduce that the transformation of smaller Cu<sub>2</sub>O nanocubes along with some Au clusters act as seeds into larger Cu<sub>2</sub>O explain the high fraction of larger Au/Cu<sub>2</sub>O particles and a small fraction of nanocubes particles observed in FESEM imaging.

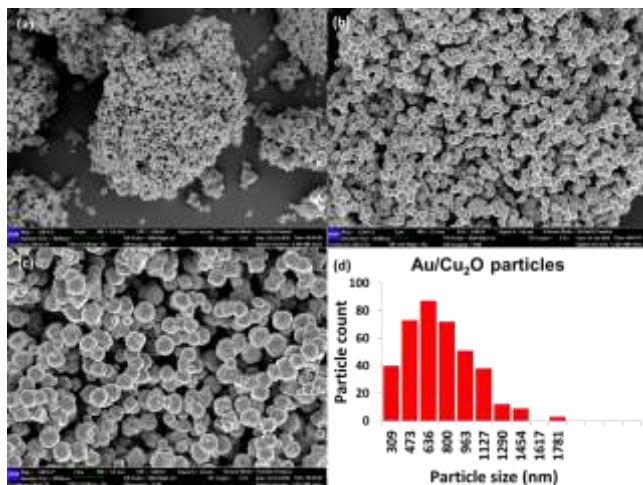


Fig. 3 (a) (b) (c) FESEM images of Au/Cu<sub>2</sub>O and (d) Histogram of the particle size distribution of Au/Cu<sub>2</sub>O

### 3.4 Optical analysis

Fig. 4(a) shows the absorption spectra of Cu<sub>2</sub>O and Au/Cu<sub>2</sub>O samples. Wide-range absorption spectra between 220 and 800 nm could be observed for both Cu<sub>2</sub>O and Au/Cu<sub>2</sub>O. The optical band gaps of Cu<sub>2</sub>O and Au/Cu<sub>2</sub>O samples were determined using the Tauc equation. Fig. 4(b) and (c), and (d) show the  $(\alpha h\nu)^2$  versus  $h\nu$  plot used to evaluate the Cu<sub>2</sub>O and Au/Cu<sub>2</sub>O band gaps by extrapolating the x-axis. The band gaps of Cu<sub>2</sub>O and

Au/Cu<sub>2</sub>O were identified as 1.93 and 1.90 eV, respectively. The bandgap of both Cu<sub>2</sub>O samples is consistent with the value found in the literature [15,18]. The decrease in the bandgap was a result of the composite formation between Au and Cu<sub>2</sub>O. The incorporation of Au<sub>9</sub> clusters onto the surface of Cu<sub>2</sub>O changed the band gap slightly. The absorbance spectrum also does not show the presence of localized surface Plasmon resonance (LSPR) indicating that the gold particle size is less than 2 nm [19].

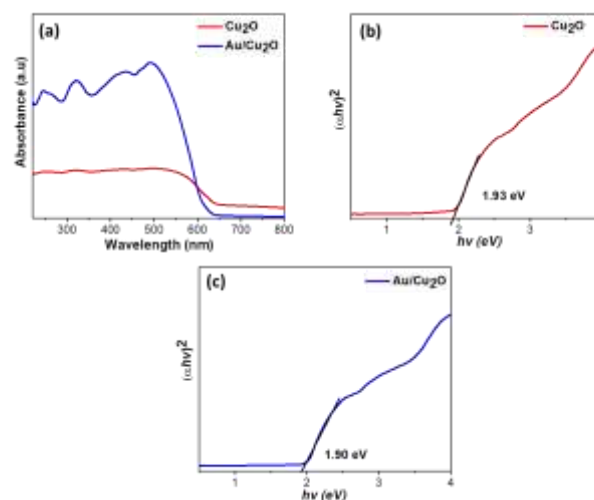


Fig. 4 UV-Vis-NIR absorption spectra of (a) Cu<sub>2</sub>O and Au/Cu<sub>2</sub>O, Tauc's plot of (b) Cu<sub>2</sub>O (c) Au/Cu<sub>2</sub>O

### 3.5 FT-IR analysis

Fig. 5 illustrates the FTIR spectra of the synthesized Cu<sub>2</sub>O and Au/Cu<sub>2</sub>O samples, the bands at 614, 701, and 827 cm<sup>-1</sup> are attributed to the Cu-O vibration. The bands at 3400 and 1622 cm<sup>-1</sup> correspond to the OH vibration. The bands at 1100, 1182, and 1380 cm<sup>-1</sup> are attributed to the C-O stretching.

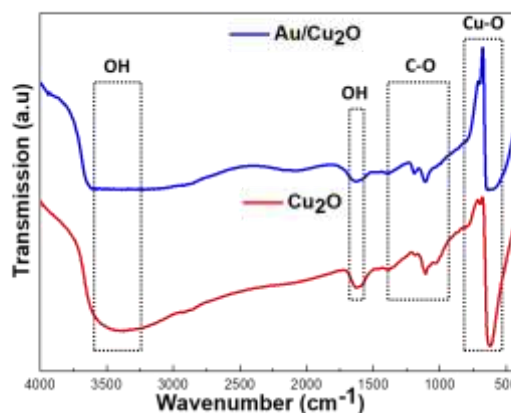


Fig. 5 FTIR spectra of Cu<sub>2</sub>O and Au/Cu<sub>2</sub>O

These results prove the existence of  $\text{Cu}_2\text{O}$ , and no bands related to  $\text{CuO}$  at 588, 534, and  $480\text{ cm}^{-1}$  appeared [9]. However, for the  $\text{Au}_9/\text{Cu}_2\text{O}$  spectrum, it can be seen that the characteristic bands at 2078, 1190, 1107, 700, and  $615\text{ cm}^{-1}$  slightly differ from that of  $\text{Cu}_2\text{O}$  which may be attributed to the presence of that small quantity of dopant [15].

### 3.6 Photoluminescence analysis

PL was done to test the rate of recombination of the photogenerated charge carriers in the  $\text{Cu}_2\text{O}$  and  $\text{Au}/\text{Cu}_2\text{O}$  samples. The result shown in Fig. 6 shows the PL spectra of pure  $\text{Cu}_2\text{O}$  and  $\text{Au}/\text{Cu}_2\text{O}$  composite under 340 nm excitation.  $\text{Cu}_2\text{O}$  shows a strong emission peak centered at around 450 to 570 nm. However, after the introduction of the Au cluster, the PL intensity was significantly quenched, which implies the lowest rate of regeneration of the photo-induced electron and hole as a result of the  $\text{Au}/\text{Cu}_2\text{O}$  formation [15,20].

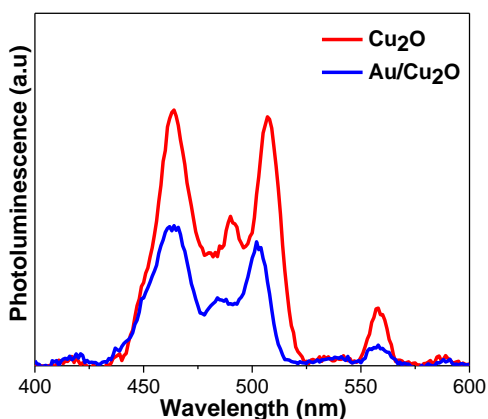


Fig. 6 PL spectra of  $\text{Cu}_2\text{O}$  and  $\text{Au}/\text{Cu}_2\text{O}$

### 3.7 Kinetics of the photocatalytic reaction

The rate of the photocatalytic degradation of MO and CR on  $\text{Au}/\text{Cu}_2\text{O}$  was obtained from the plot of individual concentrations versus their respective time. The degradation of both MO and CR was tested with all the integrated rate laws however only zero-order kinetics showed a linear relationship in all the two cases (MO and CR). As shown in Fig. 7 for CR all the concentrations give a straight line that fits well, likewise in the case of MO degradation the linear plot is only observed in zero-order kinetics. Hence, the kinetics study of the rate of degradation of MO and CR in the presence of  $\text{Au}/\text{Cu}_2\text{O}$  followed zero-order kinetics. The plot of line  $C_t$  against time showed a linear relationship and the rate constant ( $k$ ) was determined from the gradient. The calculated  $k$  for the

degradation reaction of MO is  $0.096\text{ M min}^{-1}$  while the  $k$  for the degradation of CR was found to be  $0.144\text{ M min}^{-1}$ .

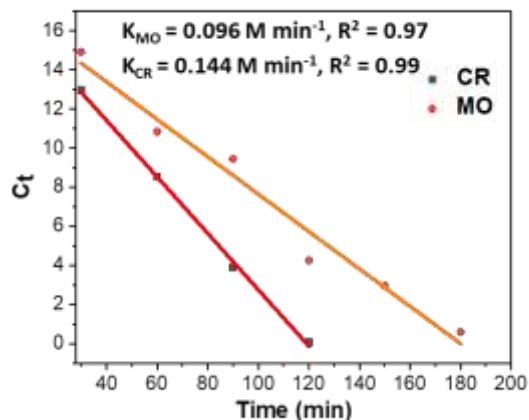


Fig. 7 Photodegradation kinetics of MO and CR dyes

## 4. CONCLUSION

$\text{Cu}_2\text{O}$  and  $\text{Au}/\text{Cu}_2\text{O}$  photocatalysts with excellent photocatalytic activity were synthesized via a simple new chemical reduction method. The  $\text{Au}/\text{Cu}_2\text{O}$  demonstrated very good photocatalytic activity on MO and CR dyes under visible light irradiation. This can be due to the effective charge separation achieved, as demonstrated by the decreased PL intensity because of the composite formation. The findings are of practical importance for photocatalysis.

## REFERENCES

- [1] R.G. Saratale, G.D. Saratale, J.S. Chang, S.P. Govindwar, J. Taiwan Inst. Chem. Eng. 42 (2011) 138–157.
- [2] S. Benkhaya, S. M'rabet, A. El Harfi, Inorg. Chem. Commun. 115 (2020) 107891.
- [3] C. Fu, M. Li, H. Li, C. Li, X. guo Wu, B. Yang, J. Alloys Compd. 692 (2017) 727–733.
- [4] N.T. Nandhini, S. Rajeshkumar, S. Mythili, Biocatal. Agric. Biotechnol. 19 (2019) 101138.
- [5] S. Mani, R.N. Bharagava, Springer New York LLC, 2016: pp. 71–104.
- [6] C.N.C. Hitam, A.A. Jalil, J. Environ. Manage. 258 (2020) 110050.
- [7] C.Y. Toe, J. Scott, R. Amal, Y.H. Ng, J. Photochem. Photobiol. C Photochem. Rev. (2018) 1–21.
- [8] Y. Su, H. Li, H. Ma, J. Robertson, A. Nathan, ACS Appl. Mater. Interfaces. 9 (2017) 8100–8106.
- [9] M. Muthukumar, S. Niranjani, K.S. Barnabas, V. Narayanan, T. Raju, K. Venkatachalam, Mater. Today Proc. 14 (2019) 563–568.
- [10] C.H. Kuo, M.H. Huang, Nano Today. 5 (2010) 106–116.
- [11] Y.H. Zhang, X.L. Cai, Y.L. Li, M.M. Liu, C.L. Ding, J.L. Chen, S.M. Fang, Chem. Phys. Lett. 734 (2019) 136748.
- [12] C. Ma, Z. Yang, W. Wang, M. Zhang, X. Hao, S. Zhu, S. Chen, J. Mater. Chem. C. 8 (2020) 2888–2898.

- [13] R.H. Adnan, G.G. Andersson, M.I.J. Polson, G.F. Metha, V.B. Golovko, *Catal. Sci. Technol.* 5 (2015) 1323–1333.
- [14] S.P. Lim, A. Pandikumar, N.M. Huang, H.N. Lim, *RSC Adv.* 5 (2015) 44398–44407.
- [15] R. Chen, J. Lu, S. Liu, M. Zheng, Z. Wang, *J. Mater. Sci.* 53 (2018) 1781–1790.
- [16] S. Sun, X. Song, Y. Sun, D. Deng, Z. Yang, *Catal. Sci. Technol.* 2 (2012) 925–930.
- [17] S. Sun, H. Zhang, X. Song, S. Liang, C. Kong, Z. Yang, *CrystEngComm.* 13 (2011) 6040–6044.
- [18] G.Z. Yuan, C.F. Hsia, Z.W. Lin, C. Chiang, Y.W. Chiang, M.H. Huang, *Chem. - A Eur. J.* 22 (2016) 12548–12556.
- [19] J.Y. Ruzicka, F. Abu Bakar, C. Hoeck, R. Adnan, C. Mcnicoll, T. Kemmitt, B.C. Cowie, G.F. Metha, G.G. Andersson, V.B. Golovko, *J. Phys. Chem. C.* 119 (2015) 24465–24474.
- [20] Y. Qu, P. Zhang, J. Liu, L. Zhao, X. Song, L. Gao, *Mater. Chem. Phys.* 226 (2019) 88–94.